A novel mitigation mechanism for photo-induced trapping in an anthradithiophene derivative using additives

Iyad Nasrallah*[1], Mahesh Kumar Ravva[2,3], Katharina Broch[4], Jiri Novak[5], John Armitage[1], Guillaume Schweicher[1], Aditya Sadhanala[1], John E. Anthony[6], Jean-Luc Bredas[2,7], Henning Sirringhaus*[1]

[1] Optoelectronics Group, Cavendish Laboratory, University of Cambridge, JJ Thomson Avenue, Cambridge, CB3 0HE, United Kingdom

[2] Division of Physical Sciences and Engineering, King Abdullah University of Science and Technology – KAUST, Thuwal 23955-6900, Kingdom of Saudi Arabia

[3] Department of Chemistry, SRM University – AP, Amaravati, 522503, India

[4] Institute for Applied Physics, University of Tuebingen, Auf der Morgenstelle 10, 72076 Tuebingen, Germany

[5] Department of Condensed Matter Physics and CEITEC, Masaryk University, Kotlarska 2, CZ-611 37 Brno, Czech Republic

[6] Department of Chemistry, University of Kentucky, Lexington, Kentucky 40506, United States

[7] School of Chemistry & Biochemistry, Georgia Tech, Atlantic Drive, Atlanta, GA 30332-0400, United States

We report a novel trap mitigation mechanism using molecular additives, which relieves a characteristic early turn-on voltage in a high-mobility *p*-type acene-based small-molecule organic semiconductor, when processed from hydrous solvents. The early turn-on voltage is attributed to photo-induced trapping, and additive incorporation has been found to be very effective in supressing this effect. Remarkably, the molecular additive does not disturb the charge transport properties of the small-molecule semiconductor, but rather intercalates in the crystal structure. This novel technique allows for the solution-processing of small molecular semiconductors from hydrous solvents, greatly simplifying manufacturing processes for large-area electronics. Along with various electric and spectroscopic characterisation techniques, simulations have given a deeper insight into the trap mitigation effect induced by the additive.

Over the last 20 years organic semiconductors have experienced impressive performance improvements. As field-effect mobilities have exceeded values of 1 cm^2/Vs, organic semiconductor based field-effect transistors (FETs) have emerged as a viable thin film electronic technology to realize displays, electronic circuits and sensors on low temperature plastic substrates [1–4]. To enable such applications a detailed understanding of the reliability of organic semiconductors under typical operational and environmental conditions and the

mechanisms that can lead to device degradation during operation is required [5–8]. There have been reports in the literature on instabilities of small-molecule based organic transistors such as pentacene to light and oxygen [9–16]. Other instabilities have been investigated, arising from trace gases in the atmosphere [17]. Few studies have been concerned with finding solutions to mitigate these instabilities. We present a simple and generally applicable additive-based technique that reduces the light-induced degradation of small-molecule based organic FETs.

2,8-difluoro-5,11-bis(triethylsilylethynyl)anthradithiophene (diF-TES ADT) - a *p*-type small molecule (SM) organic semiconductor - is a prototypical molecular semiconductor that has been widely studied owing to its high crystallinity and reproducible high charge mobilities [18]. Its high solubility in a broad range of solvents renders it easy to process by solution-based coating.

We fabricate our devices in a top-gate bottom-contact (TGBC) transistor architecture using CYTOP as gate dielectric in a nitrogen glove box environment. Air exposure during fabrication is minimal. The devices are measured in an inert atmosphere glovebox and under orange lighting (>590nm). When using ordinary mesitylene as a solvent, i.e. when no attempt was made to reduce the residual water content of the solvent, we noticed that as-fabricated diF-TES ADT FETs initially exhibit a positive turn-on voltage > 10 V, when they were first tested in the glovebox (Fig. 1a). This is observed in other literature on this small-molecule as well [19,20]. When the transistor is placed and tested in the dark and in vacuum, the turn-on voltage recovers to 0V, with the majority of the recovery taking place in the first 5 hours. Whilst in vacuum, the positive turn-on voltage is reinstated upon subsequent light illumination and removed again in the dark. This light-induced instability, which has been widely reported when exposing acene-based small-molecule FETs is seen when our transistors are exposed to orange, white and UV light (Supporting Material 1). Our optical setup does not have sufficient spectral resolution to determine whether with orange light, which is close to the bandgap of diF-TESADT, the process involves regular HOMO-LUMO excitations or specific trap states within the bandgap, but the light-induced device instability exhibit similar qualitative characteristics independent of excitation wavelength. This instability has been attributed in literature to trapping of light-generated electrons in deep trap states within the organic semiconductor bandgap. The associated trapped electrons act as a fixed negative charge near the semiconductor-dielectric interface and result in a positive shift of the turn on/threshold

voltage. In the dark the electrons slowly recombine with injected mobile holes and the positive turn-on voltage shift recovers [9–16]. The instability is undesirable for display and electronic applications - though it may be useable for light sensing applications [21,22] - and techniques are needed to minimize it.

We noticed that when processing diF-TES ADT from an anhydrous solvent, the turn-on in the as-fabricated transistors is close to 0V when measured under the same orange lighting and inert environments. Figure 1b shows the difference between a transistor fabricated from hydrous mesitylene and another fabricated from anhydrous tetralin, measured in an inert atmosphere glovebox and under orange lighting. The mesitylene device exhibits a distinct subthreshold bump and a positive turn-on voltage of around +25V in the transfer characteristics, while the tetralin device has a more regular transfer characteristic with a turn-on closer to 0V. Unfortunately, it is laborious to obtain anhydrous mesitylene, and we were unable to purchase it commercially. For a more direct comparison and to eliminate the effect the solvent itself may have, Figure 1c contrasts transistors processed from hydrous and anhydrous toluene, showing a similar difference, i.e. the device fabricated from the hydrous solvent has a more positive turn-on voltage. After the exposure of both preparations to a day in air, it is evident that the turn-on begins to drift to more positive values in both cases. This finding, as well as the one from hydrous mesitylene (Fig. 1a) provide an indication that the water/oxygen content of the film is a contending culprit to the mechanism.

We have recently demonstrated a simple method to drastically improve the operational and environmental stability of a wide range of polymer semiconductor systems, and alleviate the effect of water-induced trapping through the incorporation of small molecular additives into the semiconducting polymer films [5]. Here we adopted a similar approach by analogy to investigate whether the incorporation of a small molecular additive into the diF-TES ADT films may reduce the concentration or effectiveness of water impurities in the film and in this way improve the positive turn-on instability illustrated in Figure 1.

7,7,8,8-Tetracyanoquinodimethane (TCNQ) and 2,3,5,6-Tetrafluoro-7,7,8,8-tetracyanoquinodimethane (F4TCNQ) were used as additives in the hydrous mesitylene solution of diF-TES ADT. They are added in solution at 2 wt.%. In the case of F4TCNQ, the electron affinity is deep enough to induce *p*-type doping of diF-TES ADT, which results in a large positive turn-on voltage shift and difficulty in turning-off the devices (Fig. 2a). However,

in contrast, the addition of TCNQ successfully suppresses the positive turn-on voltage, when measured in an inert glovebox under orange lighting conditions. The literature value of the electron affinity of TCNQ (2.8-3.3 eV) [23] is significantly shallower than the HOMO of diF-TES ADT (5.3 eV) [24], and hence very little to no charge transfer doping occurs. The addition of TCNQ clearly leads to a device with near perfect turn-on near 0V even when using a hydrous solvent.

Photothermal Deflection Spectroscopy (PDS) (Fig. 2b) carried out on the preparations in Fig. 2a shows a broad polaronic absorption background signal below 2.1 eV in the case of the F4TCNQ additive (blue) due to *p*-type charge transfer doping. This is not evident in the case of TCNQ (orange), which shows no such doping effect. This is fully consistent with the electrical measurements and the energy levels of TCNQ and diF-TESADT. However, both preparations show a similar sub-bandgap absorption feature with a peak around 1.1 eV and a high energy tail between 1.4-1.6 eV. The origin of this spectral feature is discussed below.

It is remarkable to see that the addition of the additives at these small concentrations does not hinder charge transport in the films. The same level of current is achieved as that of a pure diF-TES ADT film. θ-2θ X-ray Diffraction (XRD) measurements (Fig. 2c) revealed that the (00L) lamellar stacking distance between the molecular layers is slightly increased by around 0.4Å, whereas Grazing Incidence Diffraction (GID) measurements confirmed that the crystal packing of diF-TES ADT in the direction of π–π stacking remains unaffected (Supporting Material 2). This suggests that some of the additive intercalates into the film causing the lamellar distance to increase. The TCNQ most likely inserts itself in the vicinity of the alkyne side chains of diF-TES ADT creating an anisotropic lattice expansion. This does not exclude the possibility that the additive is also incorporated into grain boundaries in the film, which we are not sensitive to in X-ray measurements. We were unable to measure directly the concentration of TCNQ in the films; it could be different from the 2 wt. % that is present in solution, but the XRD lattice expansion provides clear evidence for some level of TCNQ incorporation into the films. The full width half maximum (FWHM) of the Bragg-peak at $0.4A^{-1}$ of is reduced in the films with additives compared to the neat films, which suggest an improvement in crystallinity upon additive incorporation.

Figure 2d shows that the additive completely passivates the effect of the ambient environment on the small-molecule. After exposing a transistor to 24 hours of ambient air

environment under orange lighting, complete stability is observed without any increase in the turn-on voltage to more positive values (orange line, solid to dashed). Likewise, the black transfer characteristics show the stability before and after 24 hours of exposure to orange light in a nitrogen-filled glovebox (black line, solid to dashed). This perfect stability is in contrast to the instability shown in Figure 1c, where pure transistors develop a pronounced positive turn-on voltage after similar air exposure.

Discussion

There are several sources of impurities that can be present in the thin film of the small-molecule. It is synthesized and stored in ambient air environments, which contribute oxygenated species to the film [17], whether they are permanent bonds or charge transfer complexes. Also, since the diF-TES ADT films are annealed for only 2 minutes at 100˚C, we assume there is still a solvent content. In films spun from hydrous solvents, this content will also constitute hydrated-oxygenated species, which from hereon will be referred to as hydrated species.

It is apparent from Figure 1, that the effect observed is a photo-induced effect, whereby charge is excited from the HOMO to the LUMO of diF-TES ADT when exposed to light. This excitation is affected by the existence of hydrated species in the film, as films spun from anhydrous solvents do not exhibit the light induced effect, until they are exposed to ambient environments whereby ambient oxygen and humidity begin to induce a similar effect as those films spun from hydrous solvents (Fig. 1c).

It is also concluded that it is not a requirement for the additive to undergo charge transfer with the semiconducting molecule. In the case of TCNQ addition, where no (or very little) doping is induced, an early turn-on suppression is elegantly evident in the transfer characteristic.

The mechanism of photo-induced trapping has been reported for thiophene-based semiconducting polymers [25]. We hereby report a similar effect in highly-crystalline small-molecule semiconductors. The incorporation of additives into polymer films is significantly less detrimental to charge transport due to the amorphous/semi-crystalline nature of polymer systems. We propose a mitigation method for this photo-induced trapping mechanism through the incorporation of additives into the crystalline small-molecule film,

without any hindrance to the crystalline packing of the thin film. This in turn can induce no detrimental effect on the charge transport properties of the fabricated transistors, considering an optimized amount of additive.

In the absence of hydrated species in a pure thin film, any excited charge would recover back to the HOMO once the light is removed. However as illustrated schematically in Figure 3, the presence of hydrated species forms a trap level aligned within the band-gap of the small-molecule, where the electrons favor a relaxation to this level from the LUMO, causing them to become trapped. In the case where dark environments and vacuum are introduced, Figure 1 shows that the charges de-trap with prolonged time.

When an additive such as TCNQ is introduced to the thin film, the charge favorably relaxes onto the LUMO of TCNQ as it is lower in energy (Fig. 3, ungated). Under the influence of an electric field, such as that present in operating a transistor (Fig. 3, gated), the charge on the additive recombines with the excess of holes present in the accumulation region of the transistor, allowing the turn-on to recover to an ideal behavior. This was previously not possible in the absence of the additive, where the charge was trapped more permanently on the hydrated species. The energy level of this electron state localized on the TCNQ molecule is indicated in Fig. 3 at an energy around 4.3eV. The theoretical calculations indicate that in the presence of water and oxygen molecules this energy level can be below what would be expected from the literature value of the TCNQ electron affinity. However, we note that the value of the energy of this state depends on the detailed arrangements of the cluster being considered in the calculations and should be considered an approximate value only.

In PDS, the sub-bandgap absorption seen between 0.8 eV and 1.6 eV in thin films with TCNQ consists of two assignable signatures: the peak centered at around 1.1 eV corresponds to a localised polaron-induced absorption (PIA) of diF-TES ADT and the broad high energy shoulder can be assigned to two peaks at 1.4 eV and 1.6 eV that have been attributed in the literature to the anionic species of TCNQ/F4TCNQ [26–28] (Supporting Material 5). These peaks are synonymous and we believe this to be the optical signature of a trapped electron (that was created by photoexcitation during the PDS measurement) and a localized hole polaron induced on diF-TES ADT to compensate for the negative electron charge prior to recombination.

One can imagine a scenario where the TCNQ is closely packed between the diF-TES ADT side chains, and the hydrated species are partially solvated in the residual solvent in the films. In this case, one can see that the effect of hydrous mesitylene on transistors (Fig. 1a) will be much more pronounced than that of hydrous toluene (Fig. 1c), due to toluene having much higher water solubility than that of mesitylene (Supporting Material 5), providing a better shielding against charge trapping from the diF-TES ADT to the hydrated species.

We have performed density functional theory calculations to gain more insights on the proposed mechanism. All computational details and details of model systems considered are given in Supporting Material 6. All geometries of these complexes were fully optimized without any constraints. The optimized geometries were used to carry out the excited state analysis. The hole and electron wavefunctions were obtained from the natural transition orbital analysis.

The results obtained from these calculations clearly show that that hydrated species introduce an energy level aligned to the band gap of diF-TES ADT (Supporting Material 6, Fig. 6-1). This is in agreement with the work done by Zhuo et al.[25]. In the absence of TCNQ, in the lowest excited state, the electron density is concentrated mostly on the oxygen molecule, and the hole density is predominantly on the small molecule (Figure 4). Charged oxygen molecules could react readily with water giving, OH anions, OH radicals and OOH radicals (Supporting Material, Fig. 6-3). Hydrated OH radicals and OH anion/OOH radicals have energies deeper than diF-TES ADT's LUMO and hence are likely to be the culprits of charge trapping (Figure 4).

The incorporation of TCNQ near the side chains of diF-TES ADT - as indicated by our XRD/GID measurements - yielded no charge transfer between the molecules (Supporting Material 6, Fig. 6-2), confirming our experimental results. The calculations show that in the presence of TCNQ molecules, the light-induced excited electron density resides wholly on the TCNQ molecule, whilst the hole density remains on the small molecule (Figure 4). The electrons now reside at an energy much closer to the HOMO of the small molecule (Supporting Material 6, Fig. 6-1). As a result, the trapping effect of the hydrated species is mitigated.

Operational Stability

diF-TES ADT has shown to develop a more pronounced shoulder in the off state with increased positive gate bias stress (PGBS) (Fig. 5a) when performed under orange lighting and in a nitrogen glovebox, exhibiting a threshold voltage shift (ΔVth) of 6.1V over 12 hours of stress. When the transistor was left to de-trap in the dark for 5 hours prior to stress, and the stress was performed in the dark (Fig. 5b), the effect of PGBS was minimized to a ΔVth of 1.7V, with a reduced increase in the shoulder feature. Threshold voltage extractions can be seen in Supporting Material 7. It can also be seen in Figure 5b that the transistor recovers completely to its initial state within the first hour of post-stress recovery, which is not the case in Figure 5a, even after 3 hours of recovery.

This is an indication that the light-induced trapping mechanism described in this study influences PGBS and is hampered by slow recombination rates from the hydrated impurities back into the HOMO of the semiconductor. Unfortunately, our TCNQ additive approach, which imparts improved stability of the threshold voltage under environmental and light exposure, is not effective to improve the PGBS stability. Figure 5c shows that the PGBS–induced threshold voltage shift of devices with TCNQ additive is of a similar magnitude as of devices without the additive. At this stage it is unclear why this is the case. In a regime of bias stress, where charge trapping is influenced by prolonged applied electric fields the incorporation of TCNQ may be amplifying other trapping mechanisms, such as trapping of electrons injected from the source-drain contacts. Whilst experimenting with different additives is beyond the scope of this study, future experimentation is required to understand these to discover the right additive that imparts both good light stability and operational stability.

Conclusions

We have shown that diF-TES ADT shows a pronounced positive gate turn-on voltage, when fabricated from hydrous solvents, and when exposed to ambient environments. This has been attributed to a photo-induced effect whereby excited charges are trapped onto a trap level introduced by hydrated impurities in the semiconducting film.

We have identified that the addition of small molecular additives at small concentrations (around 2 wt.%) do not hinder the crystal packing or charge transport in the small molecular crystal lattice, but rather intercalate in the film structure forming an

anisotropic lattice expansion in the out-of-plane direction. This has the beneficial effect of alleviating the photo-induced trapping mechanism without hindrance to charge transport properties.

The method by which this occurs is by a favorable relaxation of charge onto the electron-accepting TCNQ molecule, which in the presence of an electric field, donates the charge back to the HOMO level of the semiconducting molecule.

This effect has important implications on stabilizing organic semiconductor performance against the several degrading environmental factors that they are susceptible to in their pure form, making them suitable for reproducible integration into state-of-the-art applications.

From this study, we are able to begin understanding the design features of an optimal additive molecule. To achieve light stability, the additive molecule must have an electron-accepting nature, with a LUMO level deeper than the trap level introduced by the impurity in the thin film in order to introduce a favorable transition. In order to prevent a charge transfer doping effect, it is advisable that the LUMO level is also shallower than the HOMO of the organic semiconductor. Further experimentation can determine more detailed design features (shape, size, etc…) of the additive so as to generally suit a host of different small-molecule semiconductor packing motifs, and to mitigate the effects of different sources or traps in the films.

Experimental Methods

All fabrication methods were carried out under orange lighting conditions (filter transmission above 590nm). Measurements done in inert atmospheres were conducted using a nitrogen-filled glovebox.

Transistors fabricated for this study are of top-gate bottom-contact (TGBC) architecture. Apart from Figure 1a and Supporting Material 1, all transistors have a channel length (L) of 20 µm and channel width (W) of 1 mm. The substrates are fabricated on 1737 low alkali alumino-silicate glass substrates purchased from ‘Präzisions Glas & Optik GmbH’, with a spin-coated 50nm film of polyimide (spun and from 1-Methyl-2-pyrrolidone) and cured (1hr at 160 °C, then for 3 hrs at 300 °C in N_2 glovebox) for better semiconductor film formation

properties. Chromium/gold Source and drain electrodes were patterned using photolithography, and thermally evaporated at 1.5nm/25nm thicknesses, respectively. The electrodes were treated with a pentafluorobenzenethiol (PFBT) self-assembled monolayer (SAM) for enhanced contact resistance and crystallinity into the channel region[29].

Solvents used to dissolve diF-TES ADT [30] were stored in air/nitrogen for hydrous/anhydrous analogues, respectively. However, all solutions were made inside a nitrogen-filled glovebox. diF-TES ADT was spin-coated (20 wt.% solutions, 1200 rpm for 60 seconds) and annealed at 100˚C for 2 minutes inside a nitrogen-filled glovebox. CYTOP was used as a gate dielectric, and spun to achieve films of 500nm thickness. Aluminium gate electrodes were thermally evaporated at a thickness of 35nm.

PDS samples were spun on 13mm diameter water-free boro-silicate substrates (spectrosil). Measurements were carried out in a dark environment. The PDS set-up used is home-made[31], with a high level of accuracy.

X-ray Diffraction (XRD) and Grazing Incidence Diffraction (GID) spectroscopy samples were spun on similar glass/polyimide substrates as those used for transistors. Half of the substrates were covered with a PFBT-treated 6nm thin film of chromium/gold, to mimic the preferential nucleation effects of the gold electrodes in transistors. The measurements were taken on the glass/polyimide side. The sample cross-section and measurement conditions are available in Supporting Material 2. Coplanar XRD measurements on glass were performed at beamline ID3 at the European Synchrotron Research Facility (ESRF) in Grenoble, France, using a beam energy of 15.0keV (wavelength 0.83Å) with dimensions of 500um x 30um. The detector was a Maxipix 2D pixel detector with 500 pixel x 500 pixel. The distance between the sample and the detector was 77.2cm.

Optical microscope images (Supporting Material 3) were taken using an Olympus microscope with cross-polarizers on the same samples used for XRD and GID.

Charge Accumulation Spectroscopy was carried out using a home-made set-up, and is best described in Ref. [32,33].

Acknowledgements I.N. acknowledges the financial support from FlexEnable Ltd., as well as the EPSRC Centre for Innovative Manufacturing in Large-Area Electronics (CIMLAE,

EP/K03099X/1). G.S. acknowledges postdoctoral fellowship support from the Wiener-Anspach Foundation and The Leverhulme Trust (Early Career Fellowship supported by the Isaac Newton Trust). J. N. acknowledges support from MEYS Czech Republic, project CEITEC 2020 (grant no. LQ1601).

References

1. Nag, A., Mukhopadhyay, S. C. & Kosel, J. Wearable Flexible Sensors: A Review. *IEEE Sensors Journal* **17,** 3949–3960 (2017).

2. Chang, J. S., Facchetti, A. F. & Reuss, R. A Circuits and Systems Perspective of Organic/Printed Electronics: Review, Challenges, and Contemporary and Emerging Design Approaches. *IEEE Journal on Emerging and Selected Topics in Circuits and Systems* **7,** 7–26 (2017).

3. Dodabalapur, A. Organic and polymer transistors for electronics. *Materials Today* **9,** 24–30 (2006).

4. Harding, M. J., Horne, I. P. & Yaglioglu, B. Flexible LCDs Enabled by OTFT. *SID Symp. Dig. Tech. Pap.* **48,** 793–796 (2017).

5. Nikolka, M. *et al.* High operational and environmental stability of high-mobility conjugated polymer field-effect transistors through the use of molecular additives. *Nat Mater* **16,** 356–362 (2017).

6. Nicolai, H. T. *et al.* Unification of trap-limited electron transport in semiconducting polymers. *Nat. Mater.* **11,** 882–887 (2012).

7. Sharma, A. *et al.* Proton migration mechanism for operational instabilities in organic field-effect transistors. *Phys. Rev. B - Condens. Matter Mater. Phys.* **82,** 75322 (2010).

8. Anthopoulos, T. D., Anyfantis, G. C., Papavassiliou, G. C. & Leeuw, D. M. De. Air-stable ambipolar organic transistors. *Appl. Phys. Lett.* **122105,** 1–13 (2007).

9. Ogawa, S., Naijo, T., Kimura, Y., Ishii, H. & Niwano, M. Photoinduced doping effect of pentacene field effect transistor in oxygen atmosphere studied by displacement current measurement. *Appl. Phys. Lett.* **86,** 1–3 (2005).

10. Noh, Y.-Y. *et al.* Effect of light irradiation on the characteristics of organic field-effect

transistors. *J. Appl. Phys.* **100,** 94501 (2006).

11. Jeong, S. H. & Song, C. K. Energetic distribution of interface states extracted from photo-conductance of organic thin film transistors. *Org. Electron. physics, Mater. Appl.* **15,** 2599–2607 (2014).

12. Liguori, R., Aprano, S. & Rubino, A. Metastable light induced defects in pentacene. *AIP Conf. Proc.* **1583,** 212–216 (2014).

13. Park, C. B. Investigation of the device instability feature caused by electron trapping in pentacene field effect transistors. *Appl. Phys. Lett.* **100,** 1–4 (2012).

14. Liang, Y., Dong, G., Hu, Y., Wang, L. & Qiu, Y. Low-voltage pentacene thin-film transistors with Ta2 O5 gate insulators and their reversible light-induced threshold voltage shift. *Appl. Phys. Lett.* **86,** 1–3 (2005).

15. Jurchescu, O. D., Baas, J. & Palstra, T. T. M. Electronic transport properties of pentacene single crystals upon exposure to air. *Appl. Phys. Lett.* **87,** 52102 (2005).

16. Sangeeth, C. S. S., Stadler, P., Schaur, S., Sariciftci, N. S. & Menon, R. Interfaces and traps in pentacene field-effect transistor. *J. Appl. Phys.* **108,** 113703 (2010).

17. Nasrallah, I. *et al.* Effect of Ozone on the Stability of Solution-Processed Anthradithiophene-Based Organic Field-Effect Transistors. *Chem. Mater.* **26,** 3914–3919 (2014).

18. Park, S. K., Mourey, D. A., Subramanian, S., Anthony, J. E. & Jackson, T. N. High-mobility spin-cast organic thin film transistors. *Appl. Phys. Lett.* **93,** 043301 (2008).

19. Niazi, M. R. *et al.* Solution-printed organic semiconductor blends exhibiting transport properties on par with single crystals. *Nat. Commun.* **6,** 8598 (2015).

20. Takeda, Y. *et al.* Fabrication of Ultra-Thin Printed Organic TFT CMOS Logic Circuits Optimized for Low-Voltage Wearable Sensor Applications. *Sci. Rep.* **6,** 25714 (2016).

21. Noh, Y.-Y. & Kim, D.-Y. Organic phototransistor based on pentacene as an efficient red light sensor. *Solid. State. Electron.* **51,** 1052–1055 (2007).

22. Baeg, K. J., Binda, M., Natali, D., Caironi, M. & Noh, Y. Y. Organic light detectors:

Photodiodes and phototransistors. *Advanced Materials* **25,** 4267–95 (2013).

23. Zhu, G.Z., Wang, L.-S. Vibrationally resolved photoelectron spectroscopy of the tetracyanoquinodimethane (TCNQ) anion and accurate determination of the electron affinity of TCNQ. *J. Chem. Phys.* **143**, 221102 (2015).

24. Panidi *et al.*, Remarkable Enhancement of the Hole Mobility in Several Organic Small-Molecules, Polymers, and Small-Molecule:Polymer Blend Transistors by Simple Admixing of the Lewis Acid p-Dopant $B(C_6F_5)_3$. *Adv. Sci.* **5**, 1700290 (2018).

25. Zhuo, J. M. *et al.* Direct spectroscopic evidence for a photodoping mechanism in polythiophene and poly(bithiophene-alt-thienothiophene) organic semiconductor thin films involving oxygen and sorbed moisture. *Adv. Mater.* **21,** 4747–4752 (2009).

26. Pingel, P. & Neher, D. Comprehensive picture of p-type doping of P3HT with the molecular acceptor F4TCNQ. *Phys. Rev. B - Condens. Matter Mater. Phys.* **87,** 115209 (2013).

27. Duong, D. T., Wang, C., Antono, E., Toney, M. F. & Salleo, A. The chemical and structural origin of efficient p-type doping in P3HT. *Org. Electron. physics, Mater. Appl.* **14,** 1330–1336 (2013).

28. Bozio, R., Zanon, I., Girlando, A. & Pecile, C. Influence of the intermolecular charge transfer interaction on the solution and solid state infrared spectra of 7,7,8,8-tetracyanoquinodimethane (TCNQ) alkaline salts. *J. Chem. Soc. Faraday Trans. 2* **74,** 235 (1978).

29. Gundlach, D. J. *et al.* Contact-induced crystallinity for high-performance soluble acene-based transistors and circuits. *Nat. Mater.* **7,** 216–221 (2008).

30. Subramanian, S. *et al.* Chromophore Fluorination Enhances Crystallization and Stability of Soluble Anthradithiophene Semiconductors. *J. Am. Chem. Soc.* **130,** 2706–2707 (2008).

31. Kronemeijer, A. J. *et al.* Two-Dimensional Carrier Distribution in Top-Gate Polymer Field-Effect Transistors: Correlation between Width of Density of Localized States and Urbach Energy. *Adv. Mater.* **26,** 728–733 (2014).

32. Di Pietro, R. & Sirringhaus, H. High resolution optical spectroscopy of air-induced electrical instabilities in n-type polymer semiconductors. *Adv. Mater.* **24,** 3367–3372 (2012).

33. Di Pietro, R., Fazzi, D., Kehoe, T. B. & Sirringhaus, H. Spectroscopic Investigation of Oxygen- and Water-Induced Electron Trapping and Charge Transport Instabilities in n-type Polymer Semiconductors. *J. Am. Chem. Soc.* **134,** 14877–14889 (2012).

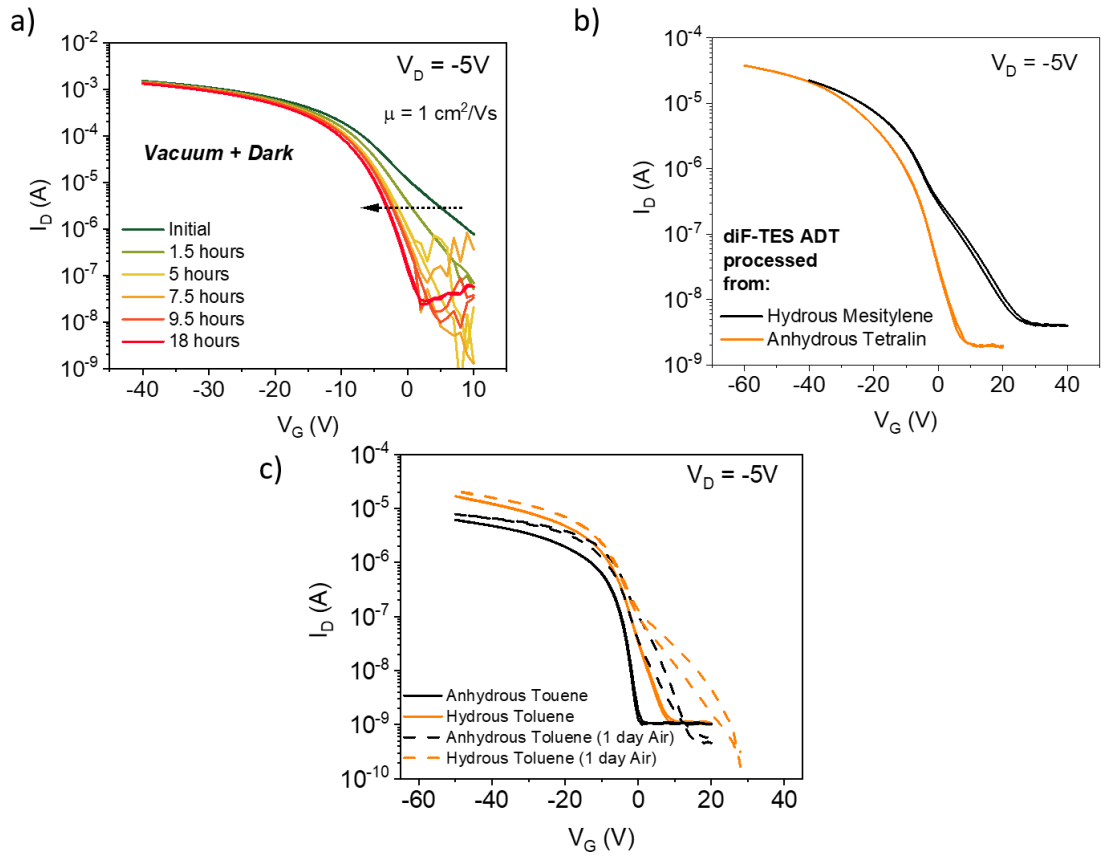

397

398

399

400 **Figure 1** a) The decrease in the gate turn-on voltage of a diF-TES ADT transistor spun from
401 hydrous mesitylene (Channel Width/Length=190 mm/80 µm), stored in the dark and in
402 vacuum. b) The difference in transfer characteristic between as-fabricated diF-TES ADT
403 transistors (Channel Width/Length=1000/20 µm) fabricated from hydrous mesitylene (black)
404 and anhydrous tetralin (orange). c) A comparison of diF-TES ADT transistors (Channel
405 Width/Length=1000/20 µm) fabricated from hydrous (orange) and anhydrous (black) toluene
406 solution, as fabricated (solid) and after a day of ambient air exposure (dashed).

407

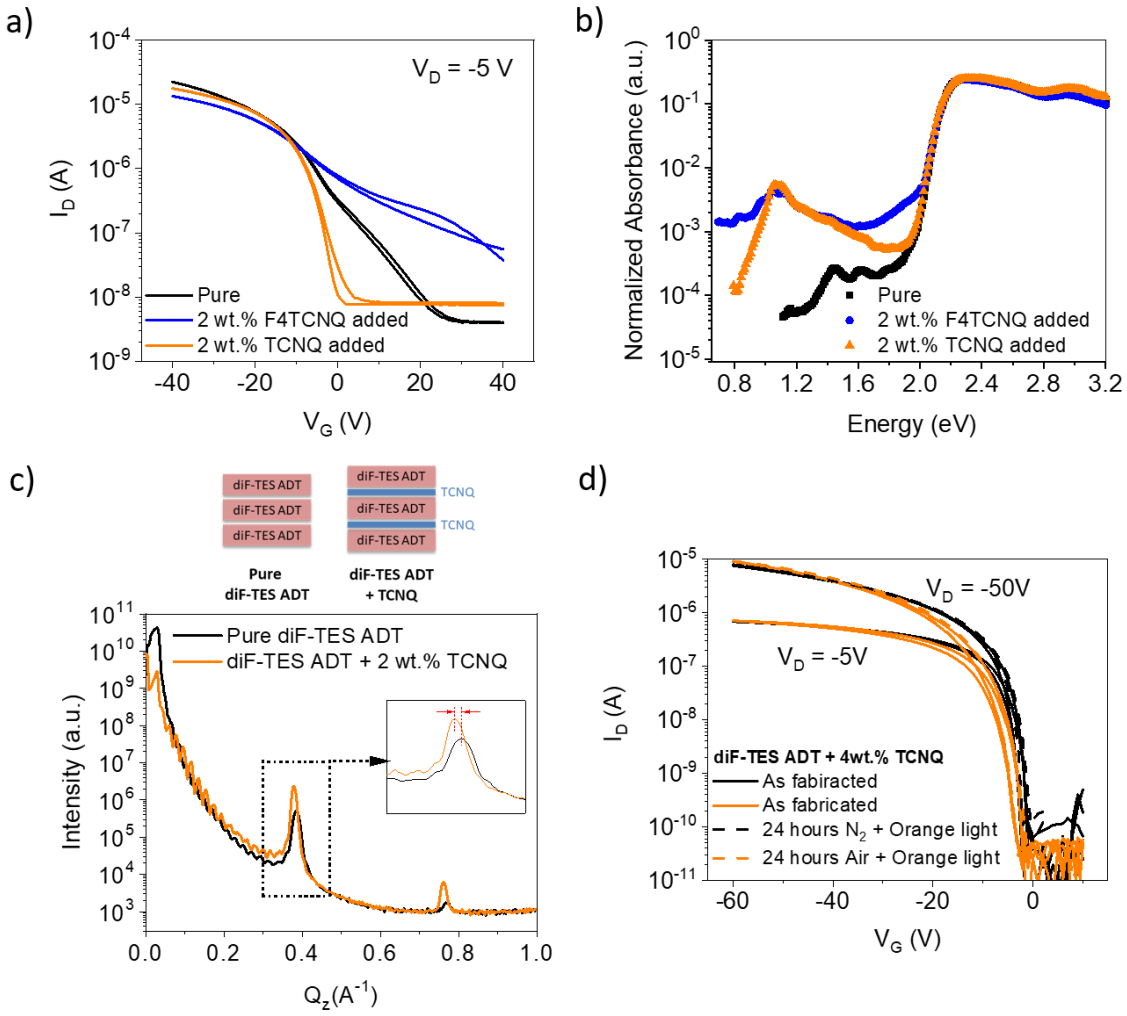

Figure 2 a) A comparison of transfer characteristics of diF-TES ADT transistors (Channel Width/Length=1000/20 µm) spun from hydrous mesitylene, pure (black), with 2 wt.% TCNQ (orange) and 2 wt.% F4TCNQ (blue). b) PDS measurements for the same preparations as those in a). c) X-ray Diffraction (XRD) curves along Q_z for pure diF-TES ADT and 2 wt.% TCNQ addition, highlighting the small z increase in the vertical spacing of diF-TES ADT packing through the addition of TCNQ. The cartoon shows the intercalation motif of TCNQ into the diF-TES ADT packing. d) Linear (V_D=-5V) and saturation (V_D=-50V) transfer characteristics (Channel Width/Length=1000/20 µm) of two transistors with 4 wt.% TCNQ. The transistor shown in orange was exposed for 24 hours to ambient air under orange lighting, while the transistor shown in black was exposed for 24 hours to orange light in a nitrogen-filled glovebox. Solid lines show the transistor before exposure, and dashed lines show the transistor after exposure, highlighting the environmental stability that TCNQ additive induces in diF-TES ADT transistors.

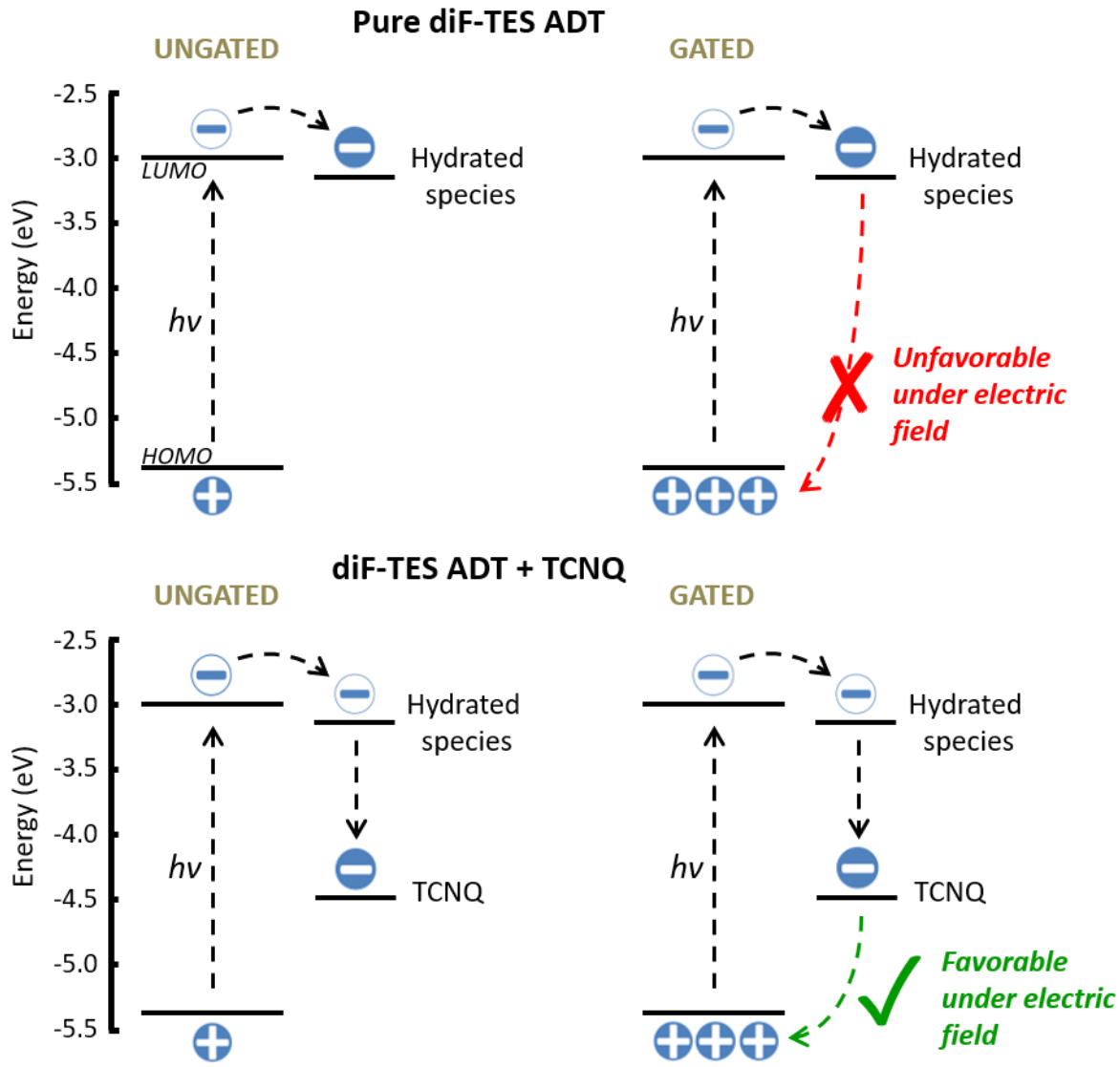

425

426 **Figure 3** The proposed mechanism by which TCNQ successfully mitigates the charge trapping
427 effect. The left two quadrants present energy level diagrams in the absence and presence
428 (top and bottom quadrant, respectively) of the TCNQ additive. The right two quadrants show
429 energy level diagrams of corresponding systems when the device is gated, and the transistor
430 channel is experiencing an electric field. The arrows denote the transfer of an electron.

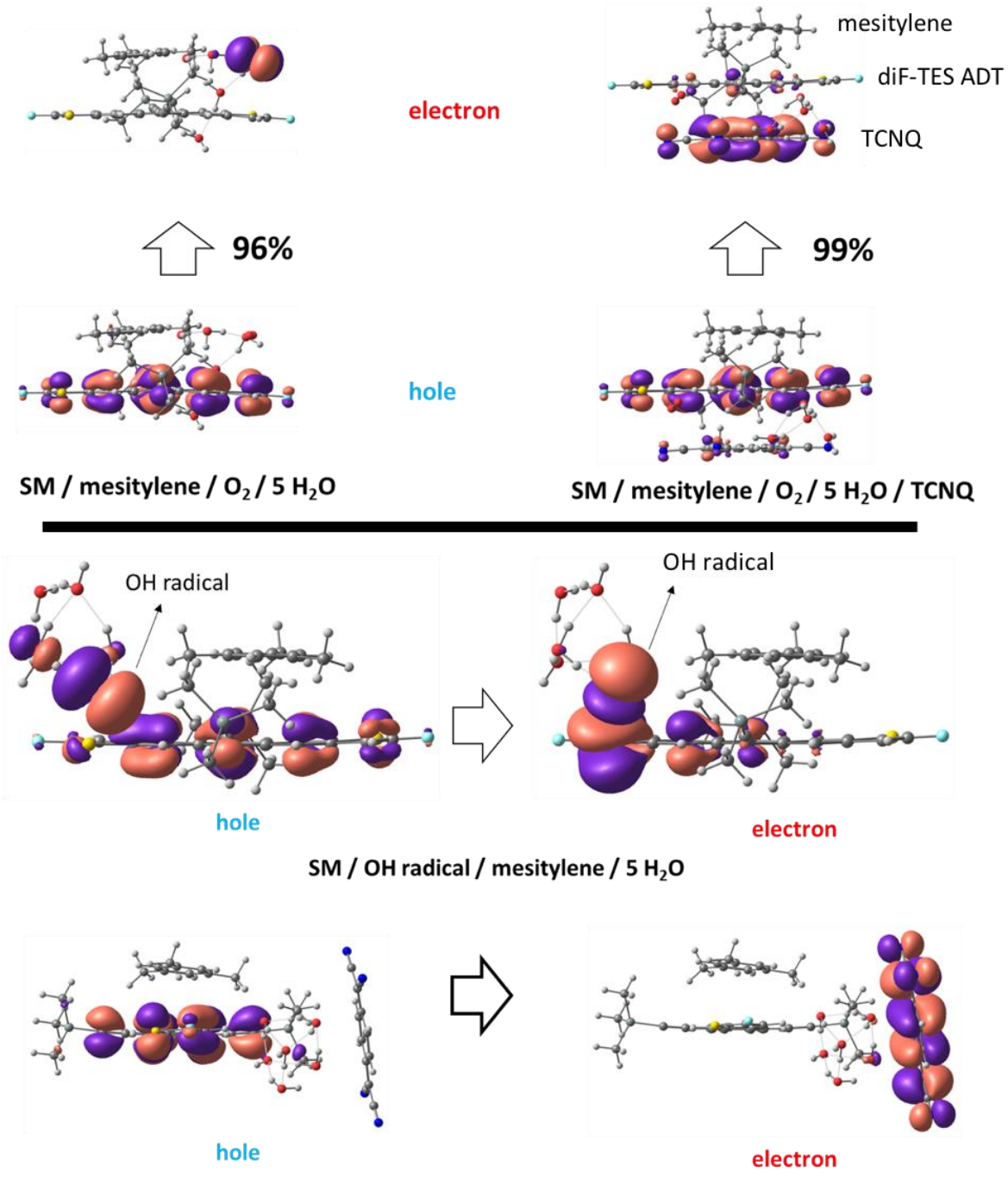

Figure 4 Pictorial representation of hole and electron wavefunctions in various clusters of the small molecule (SM) with O_2, H_2O, TCNQ and mesitylene in their lowest excited states as determined at the TD-OT(PCM)-ωB97XD/6-31G(d,p) level of theory. (Top panel) The electron density is completely on oxygen causing it to get charged. In the presence of TCNQ, the electron density is preferentially on the TCNQ. (Bottom Panel) Taking into account OH anions as a product of charged oxygen reacting with water in the film, the electron density now is on the OH anions in the absence of TCNQ, and on TCNQ when it is present. The TCNQ molecule here is placed near the side chains, as suggested by XRD.

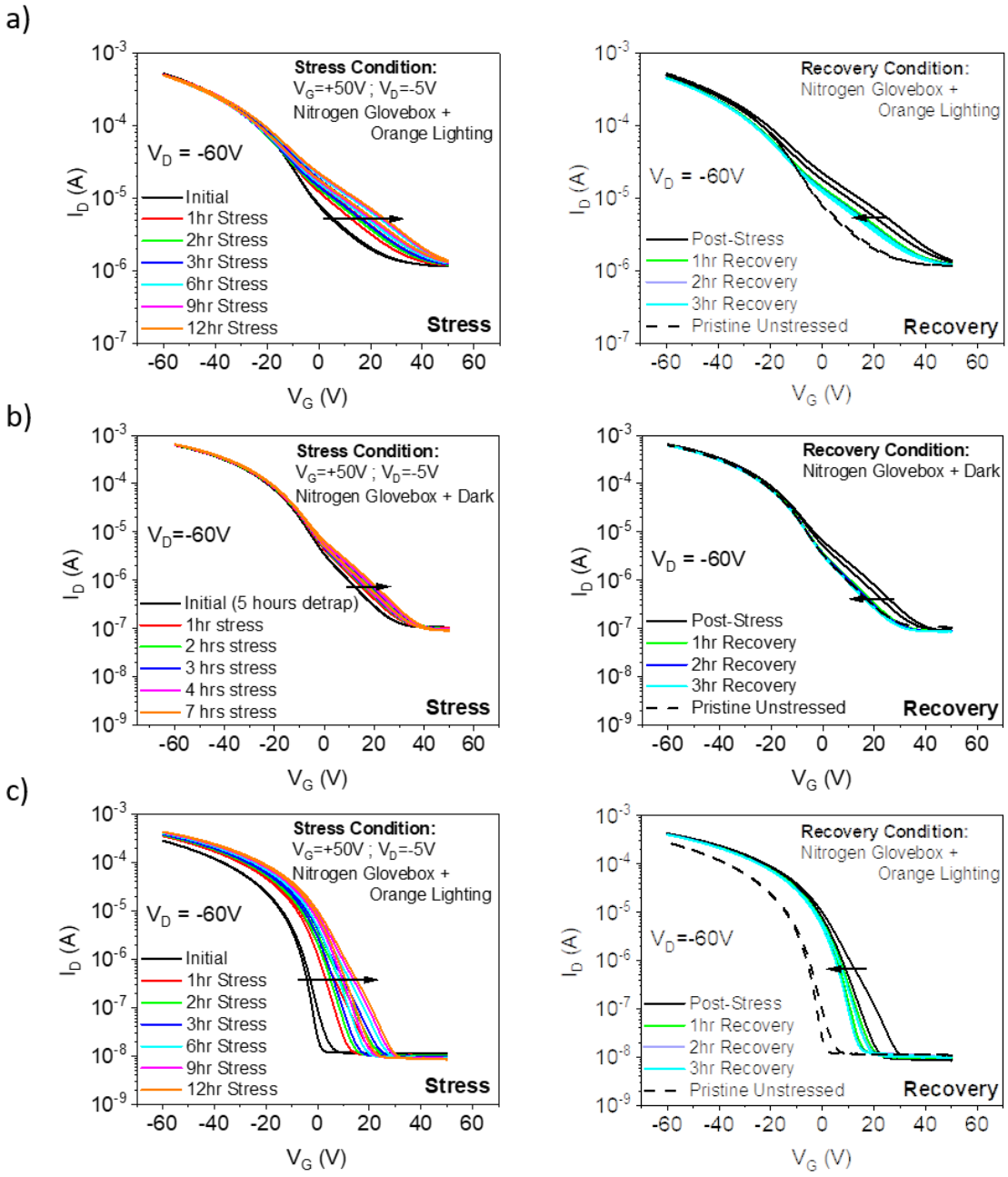

Figure 5 Transistor (Channel Width/Length=1000/20 µm) transfer characteristics showing PGBS and subsequent post-stress recovery behavior of pure diF-TES ADT in a nitrogen glovebox a) under orange lighting, b) detrapped in the dark for 5 hours prior to PGBS, with PGBS performed in the dark as well. c) shows the PGBS and post-stress recovery of diF-TES ADT with 2 wt.% TCNQ performed under orange lighting.